

## OFF-NUCLEAR AGN AS A SIGNATURE OF RECOILING MASSIVE BLACK HOLES

MARTA VOLONTERI<sup>1</sup> & PIERO MADAU<sup>2</sup>

## ABSTRACT

During the final phases of inspiral, a massive black hole (MBH) binary experiences a recoil due to the asymmetric emission of gravitational waves. We use recent results from numerical relativity simulations together with models of the assembly and growth of MBHs in hierarchical cosmologies, to study the dynamics, statistics, and observability of recoiling MBHs. We find that, at redshift  $z < 3$ , kicked non-rotating holes are typically found between 1 and 30 kpc from their galaxy centers, while rapidly rotating ones are typically between 10 and a few hundred kpc. A recoiling hole that carries an accretion disk may shine as an “off-nuclear AGN” while it moves away from the center of its host galaxy. We predict that, depending on the hole spin distribution and the duration of their active phase, a population of off-nuclear AGN may already be detectable at low and intermediate redshifts in present deep *Hubble Space Telescope* observations. The *James Webb Space Telescope* may discover tens of wandering AGN per square degree, most of them moving within their host halos on unbound trajectories.

*Subject headings:* black hole physics – cosmology: theory – galaxies: nuclei – quasars: general

## 1. INTRODUCTION

The massive black holes (MBHs) observed today at the centers of nearby galaxies (see, e.g., Richstone et al. 1998) are expected to have grown through a series of gas accretion episodes, when they shine as active galactic nuclei (AGN), and of binary coalescences following the merger of their host galaxies (e.g., Begelman et al. 1980; Volonteri et al. 2003a). Coalescing MBH pairs will give origin to the loudest gravitational wave events in the universe, and are one of the primary targets for the planned *Laser Interferometer Space Antenna* (*LISA*; e.g. Sesana et al. 2004). In general, gravitational waves also remove net linear momentum from the binary and impart a kick to the center of mass of the system. The outcome of this “gravitational rocket” has been the subject of many recent numerical relativity studies. Non-spinning holes recoil with velocities below  $200 \text{ km s}^{-1}$  that only depend on the binary mass ratio, whereas much larger kicks are predicted for rapidly rotating holes (Campanelli et al. 2007a; González et al. 2007; Herrmann et al. 2007).

If it is not ejected from the host altogether (e.g. Madau et al. 2004; Merritt et al. 2004; Haiman 2004; Volonteri & Rees 2006; Schnittman & Buonanno 2007), the recoiling MBH will travel some maximum distance and then return to the center subject to dynamical friction (Madau & Quataert 2004). Historically, MBH ejections have been proposed to explain the nature of radio jets (Saslaw et al. 1974; Valtonen & Heinämäki 2000) and trails and filaments in spiral and interacting galaxies (e.g., Arp 1976; Arp et al. 2001). Haque-Copilah et al. (1997) present a comprehensive compendium of early ideas on MBH ejections that have been recently revitalized.

Galaxy mergers are frequent at early times, so a significant number of coalescing MBH binaries is expected

to form then. Galaxy mergers are also a leading mechanism for supplying gas to their nuclear black holes, and a recoiling hole can retain the inner parts of its accretion disk, providing fuel for a continuing luminous phase along its trajectory. Two possible observational manifestations of gravitational-radiation ejection have then been suggested: (1) off-nuclear AGN activity (Madau & Quataert 2004; Loeb 2007); and (2) broad emission lines that are substantially shifted in velocity relative to the narrow-line gas left behind (Bonning et al. 2007). In this Letter we use models of the assembly and growth of MBHs in hierarchical cosmologies to study the statistics and dynamics of recoiling holes, and explore the conditions dictating their observability as off-nuclear AGN in deep optical and X-ray imaging studies.

## 2. BASIC MODEL

We follow the assembly history of dark matter halos and associated MBHs via cosmological Monte Carlo realizations of the merger hierarchy from early times to the present in a  $\Lambda$ CDM cosmology, using a model that captures many features of the MBH/AGN population (e.g., luminosity function of quasars and its evolution, black hole mass density today, stellar core formation due to MBH binary mergers). The main assumptions of the models have been discussed elsewhere (e.g. Volonteri et al. 2003a,b; Volonteri 2007 and references therein). MBHs get incorporated through halo mergers into larger and larger structures, sink to the center owing to dynamical friction against the dark matter background, and form bound binaries. The MBHs in galaxies undergoing a major merger (i.e. having a mass ratio  $> 1 : 10$ ) have masses corresponding to the  $M_{\text{BH}} - \sigma_*$  relation of their hosts, i.e. at coalescence the MBH binary mass ratio scales with the central velocity dispersions of the progenitor halos. After the formation of the binary, the black hole pair shrinks and coalesces on a timescale that is shorter than the merger time of the progenitor halos, as a result of stellar and gas-dynamical processes (e.g. Berczik et al. 2006; Mayer et al. 2007).

<sup>1</sup> Astronomy Department, University of Michigan, Ann Arbor, MI, 48109.

<sup>2</sup> Department of Astronomy & Astrophysics, University of California, Santa Cruz, CA 95064.

The recoil velocity  $\vec{V}_{\text{kick}}$  depends on the binary mass ratio  $q = M_2/M_1$ , on the dimensionless spin vectors of the pair  $\vec{a}_1$  and  $\vec{a}_2$  ( $0 < a_i < 1$ ), and on the orbital parameters. All current numerical data on kicks can be fitted by (Baker et al. 2008)

$$\vec{V}_{\text{kick}} = v_m \vec{e}_x + v_{\perp} (\cos \xi \vec{e}_x + \sin \xi \vec{e}_y) + v_{\parallel} \vec{e}_z, \quad (1)$$

$$v_m = A\eta^2 \sqrt{1 - 4\eta} (1 + B\eta), \quad (2)$$

$$v_{\perp} = H\eta^2 (1 + q)^{-1} (a_2^{\parallel} - qa_1^{\parallel}), \quad (3)$$

$$v_{\parallel} = K\eta^3 (1 + q)^{-1} \cos(\Theta - \Theta_0) (a_2^{\perp} - qa_1^{\perp}), \quad (4)$$

where  $\eta \equiv q/(1+q)^2$  is the symmetric mass ratio, the indices  $\parallel$  and  $\perp$  refer to projections parallel and perpendicular to the orbital angular momentum, respectively,  $\vec{e}_x$  and  $\vec{e}_y$  are orthogonal unit vectors in the orbital plane,  $\Theta$  is the angle between  $(\vec{a}_2^{\perp} - q\vec{a}_1^{\perp})$  and the separation vector at coalescence, and  $\Theta_0$  is some constant for a given mass ratio. Here,  $A = 1.35 \times 10^4 \text{ km s}^{-1}$ ,  $B = -1.48$ ,  $H = 7540 \pm 160 \text{ km s}^{-1}$ ,  $\xi = 215^\circ \pm 5^\circ$ , and  $K = 2.4 \pm 0.4 \times 10^5 \text{ km s}^{-1}$  (Baker et al. 2008). We will assume in the following that the orbital parameters and the spin orientations are isotropically distributed. The configuration producing the maximum recoil kick (equal-mass rapidly rotating holes with anti-aligned spins oriented parallel to the orbital plane, with the pair recoiling along the  $z$ -axis),  $V_{\text{kick}} = K\eta^3 = 3750 \text{ km s}^{-1}$ , is then quite rare (c.f. Bogdanović et al. 2007). Little

The distribution of all binary mass ratios expected in hierarchical models is found to be relatively flat (Volonteri et al. 2005). In this work we focus on binaries that could give origin to detectable off-center AGN: we therefore select pairs coalescing at  $z < 3$  with total masses  $M_1 + M_2 > 10^5 M_{\odot}$ . The distribution of mass ratios for this subsample is shown in Figure 1. For comparison, we have also derived a distribution of mass ratios by Monte Carlo sampling the  $z = 0$  MBH mass function (adopting the Schechter fit in Merloni & Heinz 2008), where we have assumed  $M_1, M_2 \in [10^4 M_{\odot}, 10^{10} M_{\odot}]$ , and we have imposed the condition  $M_1 + M_2 > 10^5 M_{\odot}$ . In the sampling of the  $z = 0$  mass function most binaries are composed of two rather small holes of similar mass, skewing the mass ratio towards unity ( $\langle q \rangle = 0.17 \pm 0.23$ , implying  $V_{\text{kick}} \sim 250 \text{ km s}^{-1}$  for  $a_i = 0.9$ ). The binary mass threshold we impose in the cosmological sampling also causes a loss of coalescing pairs with  $q \approx 1$ , because of the limited major merger activity of the corresponding host galaxies (of order of  $0.1 \text{ Gyr}^{-1}$ , White et al. 2007).

Large spins are a natural consequence of prolonged disk accretion episodes (e.g. Bardeen 1970; Volonteri et al. 2005), but can be avoided if AGN are fed by a series of small-scale, randomly oriented accretion events (King & Pringle 2005). To bracket the uncertainties, we consider here two extreme scenarios: prior to coalescence, both holes are assumed to be either non-rotating or are rapidly spinning with  $a = 0.9$ . The resulting distributions of kick velocities for these two cases are plotted in Figure 1. Close to 7% of all coalescing non-rotating holes are ejected from the nucleus with kick velocities between 100 and 200  $\text{km s}^{-1}$ ; in the spinning case, 12% get kicks above 100  $\text{km s}^{-1}$  and 2% above 500  $\text{km s}^{-1}$ .

### 3. DYNAMICS OF RECOILING HOLES

In our default model the host galaxy is described by two spherical mass components: a) the dark matter follows a Navarro et al. (1997) profile with median concentration  $c_{\text{med}} = 9(1+z)^{-1} (M_{\text{halo}}/8 \times 10^{12} h M_{\odot})^{-0.14}$  and scatter around the median of  $\Delta \log c = 0.14$  (Bullock et al. 2001); 2) the central stellar profile is modeled instead as an isothermal sphere with one-dimensional velocity dispersion  $\sigma_*$  and density

$$\rho_*(r) = \frac{\sigma_*^2}{2\pi G(r^2 + R_{\text{BH}}^2)}. \quad (5)$$

The velocity dispersion is related to the halo circular velocity  $V_c$  at the virial radius by  $V_c = \sqrt{2}\sigma_*$  (cf. Ferrarese 2002). We truncate  $\rho_*$  at the “bulge” radius  $R_B = 6 \text{ kpc}$  ( $\sigma_*/200 \text{ km s}^{-1}$ )<sup>2</sup>: this ensures that the stellar bulge mass within  $R_B$  is equal to  $1000 M_{\text{BH}}$  (Haring & Rix 2004), using  $M_{\text{BH}} = (10^8 M_{\odot}) (\sigma_*/200 \text{ km s}^{-1})^4$  (Tremaine et al. 2002). The stellar profile is also truncated inside a core radius  $R_{\text{BH}}$ , as stars within the gravitational sphere of influence of the hole,  $R_{\text{BH}} = GM_{\text{BH}}/\sigma_*^2$ , are bound to it and do not contribute to dynamical friction. The escape speed from such a 2-component potential can be approximated as  $v_{\text{esc}} \sim 2\sigma_* [c^2 f(c)^{-1} (1+c)^{-1} + \ln(R_B/R_{\text{BH}})]^{1/2}$ , where  $f(c) = \ln(1+c) - c/(1+c)$ . Following a kick, the radial orbit of

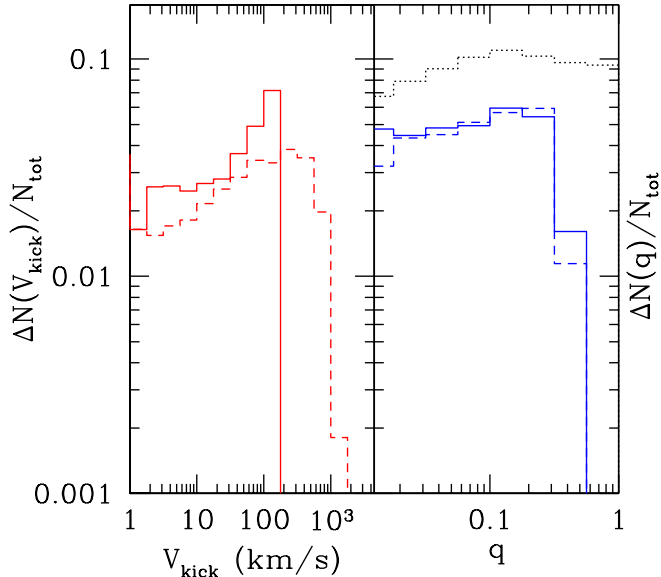


FIG. 1.— *Left panel:* Kick velocity distribution for all  $z < 3$  MBH binaries with  $M_1 + M_2 > 10^5 M_{\odot}$  in our cosmological realizations. *Solid curve:* nonspinning holes. *Dashed curve:* rapidly spinning holes with  $a_i = 0.9$ . The orbital parameters and spin vectors are assumed to be isotropically distributed. *Right panel:* distribution of binary mass ratios. *Solid curve:* nonspinning holes. *Dashed curve:* rapidly spinning holes. In the latter case more holes are ejected, and the distribution of binary mass ratios is slightly different. *Dotted curve:* Monte Carlo sampling the  $z = 0$  MBH mass function.

is known about the masses of MBH binaries and their

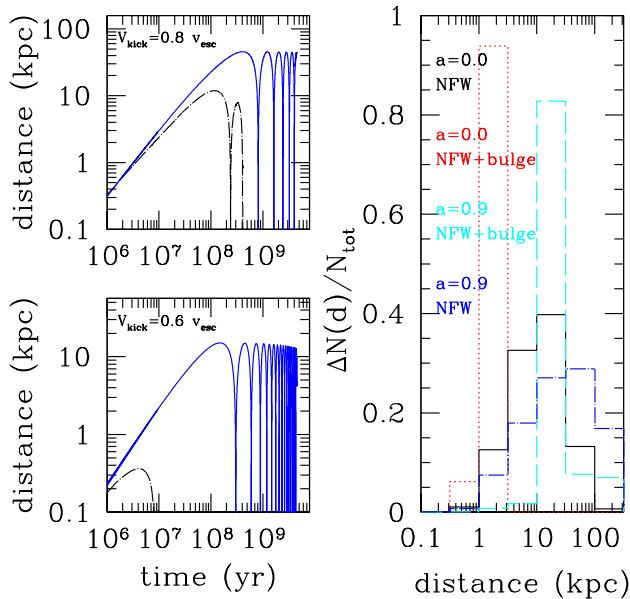


FIG. 2.— *Left panels:* Decay of a  $10^6 M_{\odot}$  MBH in a spherical halo of mass  $M_{\text{halo}} = 10^{12} M_{\odot}$  and escape velocity  $v_{\text{esc}} = 380 \text{ km s}^{-1}$ , for  $V_{\text{kick}} = 0.8 v_{\text{esc}}$  (top) and  $V_{\text{kick}} = 0.6 v_{\text{esc}}$  (bottom). *Solid curves:* orbits in a NFW+bulge potential. *Dot-Dashed curves:* orbits in a NFW potential. *Right panel:* Distributions of MBH displacements for all  $z < 3$  MBH binaries with  $M_1 + M_2 > 10^5 M_{\odot}$  in our cosmological realizations. *Solid histogram:* nonspinning holes in a NFW potential. *Dotted histogram:* nonspinning holes in a NFW+bulge potential. *Dot-Dashed histogram:*  $a = 0.9$  holes in a NFW potential. *Dashed histogram:*  $a = 0.9$  holes in a NFW+bulge potential.

a MBH in a spherical potential is governed by:

$$\frac{d^2 \vec{r}}{dt^2} = -\frac{GM(r)}{r^2} \vec{r} - \frac{4\pi G^2 \ln \Lambda \rho M_{\text{BH,tot}}}{v^2} f(x) \vec{v} \quad (6)$$

where  $f(x) \equiv [\text{erf}(x) - (2x/\sqrt{\pi})e^{-x^2}]$ ,  $x \equiv v/\sqrt{2}\sigma$ , and the velocity dispersion  $\sigma$  is derived from the Jeans' equation for the composite profile, assuming isotropy (e.g. Binney & Tremaine 1987). Here  $M(r)$  describes the total mass of the host galaxy within  $r$ ,  $\rho(r)$  is the total density profile, and the second term represents dynamical friction against the stellar and dark matter background (e.g. Binney & Tremaine 1987). Stars and gas bound to the hole are displaced with it: here we assume, in first approximation (see below), that the total ejected mass is  $M_{\text{BH,tot}} = 2M_{\text{BH}}$ . The Coulomb logarithm,  $\ln \Lambda$ , in equation (6) is taken equal to 2.5 (Gualandris & Merritt 2007).

A MBH ejected with  $V_{\text{kick}} < v_{\text{esc}}$  will oscillate about the nucleus losing orbital energy via dynamical friction (Madau & Quataert 2004). Note, however, that the assumption that the central stellar density profile is unmodified by the heating effect of dynamical friction tends to artificially shorten the MBH decay timescale (Boylan-Kolchin et al. 2004). Moreover, while in a spherical potential the hole will remain on a purely radial orbit, in a realistic triaxial galaxy the hole acquires angular momentum and does not return through the dense center. This is known to reduce the effect of friction and to increase the decay time by a factor of a few relative to the spherical case (Vicari et al. 2007). To approximate the

delaying effect of a triaxial geometry and of a decreasing core density, we have also run a case in which MBHs move in in a bulgeless pure NFW potential. The two left panels in Figure 2. show two examples of orbital decays (for  $V_{\text{kick}} = 0.6, 0.8 v_{\text{esc}}$ ) in a NFW+bulge (“short decay”) and NFW only (“long decay”) model. The right panel depicts the ensuing distributions of MBH displacements, with and without spin. In all but the NFW+bulge  $a = 0$  case, a significant fraction of recoiling holes are found between 10 and 100 kpc from their galaxy centers (at redshift 2, a displacement of 10 kpc corresponds to an angular size of 1.2 arcseconds). Note that, in our realizations, only 0.1-0.3% of all MBHs at a given cosmic epoch are actually off-center.

#### 4. OFF-NUCLEAR AGN

A recoiling hole that carries an accretion disk may be detected as it moves away from the center of its host. To assess the detectability of a subpopulation of off-nuclear AGN in deep imaging survey, we assume that all recoiling holes accrete at a fraction  $f_E$  of the Eddington rate  $\dot{M}_E = 4\pi GM_{\text{BH}} m_p / c\sigma_T$ ,  $L = \epsilon f_E L_E$ , with radiative efficiency  $\epsilon$ . The rest-frame optical part of their spectrum is modelled as a multicolor Shakura & Sunyaev (1973) disk with maximum temperature  $kT_{\text{max}} \sim 1 \text{ keV} (M_{\text{BH}}/M_{\odot})^{-1/4}$ , following a power-law with  $L_{\nu} \sim \nu^{1/3}$  at  $h\nu < kT_{\text{max}}$ . The X-ray spectral energy distribution is described by a power-law with photon index  $\Gamma = 1.9$  and an exponential cutoff at 500 keV (Marconi et al. 2004). The duration of the luminous phase depends on the amount of disk material out to the radius  $R_{\text{out}} \approx GM_{\text{BH}}/V_{\text{kick}}^2$  that is carried by the hole. In the case of an  $\alpha$ -disk, this is given by (Loeb 2007)

$$M_{\text{disk}} \approx (1.9 \times 10^6 M_{\odot}) \alpha_{-1}^{-0.8} (\epsilon_{-1}/f_E)^{-0.6} M_7^{2.2} V_3^{-2.8}, \quad (7)$$

where  $\epsilon_{-1} \equiv \epsilon/0.1$ ,  $M_7 \equiv M_{\text{BH}}/10^7 M_{\odot}$ ,  $V_3 \equiv V_{\text{kick}}/10^3 \text{ km s}^{-1}$ , and  $\alpha_{-1} \equiv \alpha/0.1$  is the viscosity parameter. The condition  $M_{\text{disk}} \leq M_{\text{BH}}$  requires

$$V_{\text{kick}} \geq 550 \text{ km s}^{-1} \alpha_{-1}^{-0.28} (\epsilon_{-1}/f_E)^{-0.21} M_7^{0.43}. \quad (8)$$

When the above equation is not satisfied, we impose  $M_{\text{disk}} = M_{\text{BH}}$  corresponding to an AGN lifetime of  $t_{\text{max}} = \epsilon c\sigma_T / (4\pi G m_p f_E) \approx 4.5 \times 10^7 \text{ yr} (\epsilon_{-1}/f_E)$ . A hole/disk system with  $(M_7, \alpha, \epsilon, f_E, M_{\text{disk}}) = (1, 0.1, 0.1, 1, M_{\text{BH}})$  recoiling with  $V_{\text{kick}} = 500 \text{ km s}^{-1}$ , could then still be shining as far as 30 kpc away of the center of its host and appear as an off-center quasar.

Figure 3 shows the expected number of detectable off-center AGN in deep and large surveys such as the *Chandra* Deep Field North and *HST*-COSMOS, and the predicted counts for future observations with the *JWST*. We set the minimum resolvable separation between a recoiling MBH and its galaxy centroid to twice the telescope resolution (i.e. 0.2 arcsec for *HST* and *JWST*, 1 arcsec for *Chandra*). We do not correct our counts for obscuration or Compton thick sources. In the *HST*-COSMOS fields (2 square degrees) we expect  $\sim 30$  sources for the best case of large kicks (spinning holes), long decay timescales (no bulge), and long active phase ( $f_E=0.1$ ,  $\alpha=0.01$ ), but less than 1 in the unfavourable cases. In the small CDF-N field we expect at most 1 off-nuclear AGN in the most

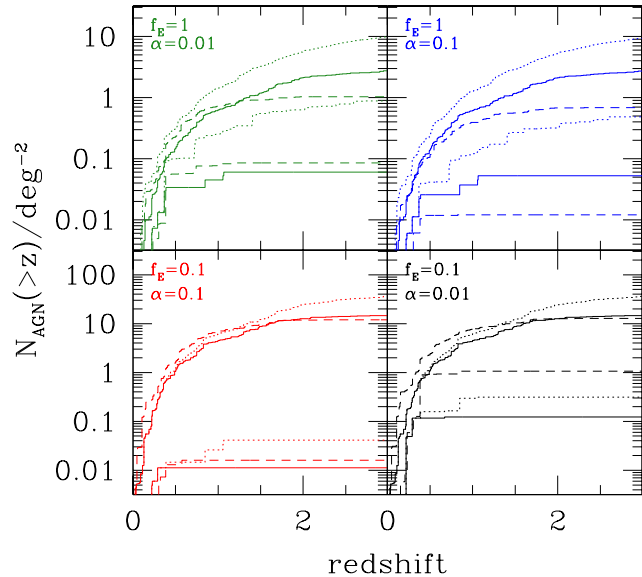


FIG. 3.— Cumulative number counts of off-nuclear AGN detectable by the *HST*, *Chandra*, and the *JWST*. *Solid curve*: number counts at the sensitivity limit of the HST-COSMOS survey. *Dashed curve*: same at the sensitivity of the CDF-N survey. *Dotted curve*: same at a *JWST* sensitivity of 10 nJy at  $2\mu\text{m}$ . In each panel the upper (lower) set of curves shows the results for a bulgeless (NFW+bulge) potential.

optimistic case, while in the  $0.77\text{deg}^2$  X-ray Chandra-COSMOS we can expect up to a few sources. Follow-up X-ray observations will be essential for the identification of the source as a genuine off-center AGN. The *JWST* yields the highest counts, about 40 sources per square degree in the best scenario.

## 5. SUMMARY

Motivated by recent numerical simulations of black hole binary coalescence and ensuing gravitational-wave

kicks, and by the large rate of MBH binary formation expected during the assembly of massive galaxies, we have assessed the detectability of recoiling holes that retain the inner parts of their accretion disk along their trajectory and shine as off-nuclear AGN. While the search for kinematically offset QSOs in the *Sloan Digital Sky Survey* (SDSS) indicates that large kicks rarely occur during a long-lasting active phase (with an upper limit on the incidence of wandering AGN with line-of-sight velocities above  $800\text{ km s}^{-1}$  of 0.2%, Bonning et al. 2007), a strong candidate for a rapidly receding MBH has been recently found in the SDSS database by Komossa et al. (2008), showing an emission line spectrum offset by  $2650\text{ km s}^{-1}$  (but see Bogdanovic et al. 2008, Dotti et al. 2008 for a different interpretation). Here, we have traced the formation history of MBH binaries in galaxies through cosmological Monte Carlo realizations of the halo merger tree, assigned a kick velocity to every MBH binary coalescence expected in our simulation, followed the orbital evolution of the ejected hole in the potential of the host, and determined the duration of a off-nuclear AGN phase on scales that can be resolved by current and future optical, IR, and X-ray satellites. The basic conclusion of this Letter is that, depending on the hole spin distribution and the duration of their active phase, a population of off-nuclear AGN may already be detectable at low and intermediate redshifts in present deep *HST* observations. The *JWST* should discover tens of wandering AGN per square degree, moving within their host halos on unbound trajectories.

Support for this work was provided by NASA grants NNG04GK85G and NNX08AV68G (P.M.) and SAO-G07-8138 C (M.V.).

## REFERENCES

- Arp, H. 1976, *ApJ*, 207, L147  
 Arp, H. C., Burbidge, E. M., Chu, Y., & Zhu, X. 2001, *ApJ*, 553, L11  
 Baker, J. G., Boggs, W. D., Centrella, J., Kelly, B. J., McWilliams, S. T., Miller, M. C., & van Meter, J. R. 2008, *ArXiv e-prints*, 802  
 Bardeen, J. M. 1970, *Nature*, 226, 64  
 Begelman, M. C., Blandford, R. D., & Rees, M. J. 1980, *Nature*, 287, 307  
 Berczik, P., Merritt, D., Spurzem, R., & Bischof, H.-P. 2006, *ApJ*, 642, L21  
 Binney, J., & Tremaine, S. 1987, *Galactic Dynamics* (Princeton: Princeton Univ. Press)  
 Bogdanović, T., Reynolds, C. S., & Miller, M. C. 2007, *ApJ*, 661, L147  
 Bonning, E. W., Shields, G. A., & Salvander, S. 2007, *ApJ*, 666, L13  
 Boylan-Kolchin, M., Ma, C.-P., & Quataert, E. 2004, *ApJ*, 613, L37  
 Bullock, J. S., Dekel, A., Kolatt, T. S., Kravtsov, A. V., Klypin, A. A., Porciani, C., & Primack, J. R. 2001, *ApJ*, 555, 240  
 Campanelli, M., Lousto, C., Zlochower, Y., & Merritt, D. 2007a, *ApJ*, 659, L5  
 Ferrarese, L. 2002, *ApJ*, 578, 90  
 González, J. A., Spherhake, U., Brüggemann, B., Hannam, M., & Husa, S. 2007, *Physical Review Letters*, 98, 091101  
 Gualandris, A. & Merritt, D. 2008, *ApJ*, 678, 780  
 Haiman, Z. 2004, *ApJ*, 613, 36  
 Haque-Copilah, S., Basu, D., & Valtonen, M. 1997, *Journal of Astrophysics and Astronomy*, 18, 73  
 Haring, N. & Rix, H.-W. 2004, *ApJ*, 604, L89  
 Herrmann, F., Hinder, I., Shoemaker, D. M., Laguna, P., & Matzner, R. A. 2007, *Phys. Rev. D*, 76, 084032  
 Hoffman, L. & Loeb, A. 2006, *ApJ*, 638, L75  
 Hopkins, P. F., Hernquist, L., Martini, P., Cox, T. J., Robertson, B., Di Matteo, T., & Springel, V. 2005, *ApJ*, 625, L71  
 King, A. R., & Pringle, J. E. 2007, *MNRAS*, 377, L25  
 Komossa, S., Zhou, H., & Lu, H. 2008, *ApJ*, 678, L81  
 Loeb, A. 2007, *Physical Review Letters*, 99, 041103  
 Madau, P. & Quataert, E. 2004, *ApJ*, 606, L17  
 Madau, P., Rees, M. J., Volonteri, M., Haardt, F., & Oh, S. P. 2004, *ApJ*, 604, 484  
 Marconi, A., Risaliti, G., Gilli, R., Hunt, L. K., Maiolino, R., & Salvati, M. 2004, *MNRAS*, 351, 169  
 Mayer, L., Kazantzidis, S., Madau, P., Colpi, M., Quinn, T., & Wadsley, J. 2007, *Science*, 316, 1874  
 Merloni, A., & Heinz, S. 2008, *MNRAS*, 388, 1011  
 Merritt, D., Milosavljević, M., Favata, M., Hughes, S. A., & Holz, D. E. 2004, *ApJ*, 607, L9  
 Navarro, J. F., Frenk, C. S., & White, S. D. M. 1997, *ApJ*, 490, 493  
 Richstone, D. et al. 1998, *Nature*, 395, A14+

- Saslaw, W. C., Valtonen, M. J., & Aarseth, S. J. 1974, *ApJ*, 190, 253
- Schnittman, J. D. & Buonanno, A. 2007, *ApJ*, 662, L63
- Sesana, A., Haardt, F., Madau, P., & Volonteri, M. 2004, *ApJ*, 611, 623
- Shakura, N. I. & Sunyaev, R. A. 1973, *A&A*, 24, 337
- Tremaine, S., et al. 2002, *ApJ*, 574, 740
- Valtonen, M. J., & Heinämäki, P. 2000, *ApJ*, 530, 107
- Vicari, A., Capuzzo-Dolcetta, R., & Merritt, D. 2007, *ApJ*, 662, 797
- Volonteri, M. 2007, *ApJ*, 663, L5
- Volonteri, M., Haardt, F., & Madau, P. 2003a, *ApJ*, 582, 559
- Volonteri, M., Madau, P., & Haardt, F. 2003b, *ApJ*, 593, 661
- Volonteri, M., Madau, P., Quataert, E., & Rees, M. J. 2005, *ApJ*, 620, 69
- Volonteri, M. & Rees, M. J. 2006, *ApJ*, 650, 669
- White, M., Zheng Z., Brown M. J. I., Dey A., & Jannuzi B. T. 2007, *ApJ*, 655, L6